

pubs.acs.org/JPCC Article

Direct Measurement of Molecular Contact Area Using Sum Frequency Generation Spectroscopy

Utkarsh Patil, ** Stephen Merriman, ** Shubhendu Kumar, ** and Ali Dhinojwala**



Cite This: https://doi.org/10.1021/acs.jpcc.4c05287



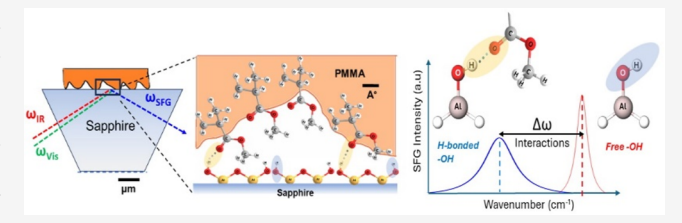
ACCESS I

III Metrics & More

Article Recommendations

Supporting Information

ABSTRACT: The molecular interactions between two solid surfaces at a subnanometer-length scale can control phenomena such as adhesion, friction, and wetting properties. These interactions, which comprise the actual contact area at the molecular scale between two materials, have historically been a challenge to measure. Here, we show the use of surface-sensitive sum frequency generation spectroscopy to probe the molecular contact between two solid surfaces that vary in roughness and



modulus. The molecular interactions are measured by a shift in the vibrational energy of surface hydroxyl groups (OH) on sapphire substrates after interacting with rough poly(methyl methacrylate) sheets. We relate the shift of the OH peak to the contact area and find a dramatic drop in the contact area with increases in roughness and modulus. In contrast, softer sheets were able to deform and create a complete mechanical contact. Interestingly, we find that complete mechanical contact alone was insufficient to maximize the molecular contact. Instead, the molecular rearrangement of interfacial molecules was necessary to enhance the interaction energy.

INTRODUCTION

When we grab a piece of paper, there is no observable adhesion between the paper and our fingers. This is due to an insignificantly small fraction of area in molecular contact between these two surfaces. Nonspecific van der Waals interactions are maximized when separation gaps are around 3-10 Å, and these interactions drop off quickly with an increase in separation.² Interactions such as hydrogen bonding are affected by an even shorter length scale than for van der Waals interactions, and this finding highlights the sensitivity and length scale needed for understanding phenomena such as adhesion, friction, and conductivity.^{3–8} The optical tools used to study contact interfaces rely on measuring the intensity of light, and any scattering of light due to roughness can limit the range of sensitivity of the optical tools to measure separation gaps of the order of tens of nanometers.9-13 Fluorescencebased techniques in combination with high-resolution microscopy give a spatial resolution of 50-100 nm and rely on changes in the intensity or wavelength of the fluorescence light to determine if the contact has been made. 14-16 Further, the technique also relies on external fluorescence molecules, and the separation length scale that we can probe without perturbing the system is constrained by the size of these molecules.

Here, we combine the sensitivity of vibrational spectroscopy to probe molecular interactions with subnanometer resolution and surface sensitivity of infrared-visible sum frequency generation spectroscopy (SFG) to probe molecular contact between two rough surfaces. SFG is employed in total internal reflection geometry to probe the interface between a sapphire prism in contact with a plastic sheet with fixed chemistry but

controlled roughness and modulus. Since SFG signals are generated only when there is a breakdown in centrosymmetry, the SFG intensity changes that occur as a function of the infrared wavelength will provide spectral information for the vibrational energies of the interfacial molecules only. ¹⁷,18

The SFG experiments were carried out using a sapphire prism in an internal reflection geometry. When SFG spectra are collected in the presence of air, a sharp OH peak is observed that corresponds to the stretching vibration of the surface sapphire OH groups. 19,20 When these sapphire OH groups encounter liquids or solids of different basicity, the OH peak shifts to lower wavenumbers. The magnitude of this shift is proportional to the interaction energy and can be related to heat of enthalpy using the Badger-Bauer rule.²¹ This interaction is short-range, and even the presence of a single layer of graphene (thickness of 0.3 nm) can disrupt this interaction with the surface OH groups.²² Therefore, the magnitude of the shift of the OH peak serves as an indicator of whether interaction has taken place with the surface OH group. We have used this sensitivity of the shift of the OH peak to quantify the strength of the interactions and related this to mechanical adhesion.²³

Received: August 5, 2024 Revised: September 4, 2024 Accepted: September 10, 2024



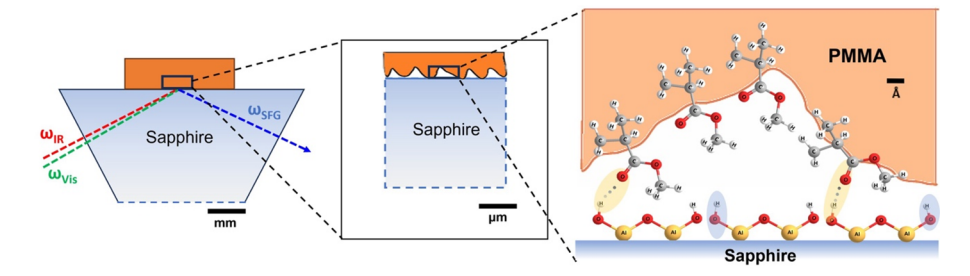


Figure 1. Schematic diagram showing the SFG setup, wherein IR (ω_{IR}) and visible (ω_{Vis}) beams are incident on the contact region. The SFG beam that originates at the surface (ω_{SFG}) was collected to give raw SFG spectra. The schematic illustrates the nature of molecular contact with the carbonyl groups (yellow) of PMMA as they interact with the surface hydroxyl groups (blue) on the sapphire substrate. These acid—base interactions are short-range interactions and are direct indicators of molecular contact.

Here, we monitor the shifts in the peak position of the OH groups, which exist as a single layer on the sapphire surface after contact with the rough plastic sheets. For regions where there is no contact with the sapphire (gaps larger than 0.3 nm), we should observe no shift of the OH peak, and at smaller separation, the magnitude of the shift of the hydroxyl group (OH) peak is directly proportional to the interaction energy.²⁴⁻²⁶ For smooth surfaces, we have shown that the interaction energy is proportional to the adhesion energy measured using contact mechanics.²³ Here, we extend this approach for the first time to quantify the molecular contact area between two rough surfaces by utilizing the fact that the interfacial interaction energy is intrinsically related to the number of molecules in contact. Ultimately, the actual molecular contact determines the properties, such as adhesion, friction, and electrical/thermal conductivity.

EXPERIMENTAL METHODS

Materials and Substrates. Poly(methyl methacrylate) (PMMA) with a molecular weight of 100 000 g/mol and a polydispersity of 1.09, which were obtained from Scientific Polymer Products (Ontario, NY, USA), was used for PMMA bilayer preparation. Additional PMMA with a molecular weight of 75 000 g/mol, obtained from Sigma-Aldrich (St. Louis, MO, USA), was used for thick PMMA sheet preparation. Sheets of polydimethylsiloxane (PDMS) were prepared according to previous reports. Sandpaper of grit size (30 grit) was obtained from 3 M Corp. (Maplewood, MN, USA). Additional chemicals of high purity were obtained from common commercial suppliers. All chemicals were used as received.

Equilateral sapphire prisms (15 mm × 15 mm × 15 mm × 10 mm; Meller Optics, Providence, RI, USA) used for SFG experiments were first cleaned by baking at 750 °C for 4 h; subjecting them to ultrasonication in toluene, acetone, and ethanol for 1 h each; and subsequently exposing them to plasma treatment for 5 min (PDC-001-HP expanded plasma cleaner; Harrick Plasma, Ithaca, NY, USA). For mechanical contact experiments, these prisms were directly used. To prepare spuncast PMMA prisms, we used a 4 wt % solution of PMMA in toluene and a rotation speed of 2000 rpm for 1 min, followed by annealing at 120 °C overnight in vacuum.

PMMA-PDMS bilayers were prepared using the film transfer procedure previously reported.^{23,28} The modulus of the chosen PDMS substrate was 1 MPa, and PMMA film (with thicknesses of either 10 or 200 nm) was transferred to the top of the substrate. Thick sheets of PMMA (PMMA "hardsheets") were prepared by compression molding of stock PMMA powder between sheets of Kapton (smooth polyimide

films) at 180 °C for 20 min under a load of 15,000 lbs to prepare a smooth surface. The final sheets, around 1 mm in thickness, were cut into pieces approximately 0.5×0.5 cm in size. For some samples, additional roughness was introduced by rubbing with a 30-grit or 1500-grit sandpaper sheet by hand with moderate pressure for 1 min. PMMA hardsheets were cleaned using ethanol and were blow-dried under N_2 flow prior to use

Roughness Characterization. The roughness values of PMMA hardsheets were measured by using a Dextax KT stylus profilometer. Scans of 0.3, 0.6, and 1 mm were collected at multiple locations using a 2 μ m tip. For soft bilayers, scans of 5 μ m, 10 μ m, 25 μ m, and 50 μ m were collected using a RTESPA 300 Tip (Bruker Corp., Billerica, MA, USA) of 8 nm nominal radius and 40 N/m stiffness using a Bruker Dimension Icon atomic force microscope (AFM).

Sum Frequency Generation Spectroscopy. Sum frequency generation (SFG) spectra were collected using a Spectra-Physics laser system, which has been described in previous work.³³ Using this system, an 800 nm visible beam and an infrared beam tunable in the range of 2000-3850 cm⁻¹ with incident angles of 8.5° and 10° , respectively, are overlapped at the surface of a sapphire prism in total internal reflection geometry. The incident angles were chosen to provide a maximum signal contribution from the PMMAsapphire contact interface based on Fresnel factor calculations. The spectra were collected in PPP polarization (i.e., ppolarized SFG, visible, and infrared beams). The prism was fitted into a custom contact cell that allowed for spectra to be collected with a sample brought into contact in situ. Experiments began by collecting a blank sapphire-air spectrum for reference followed by bringing the substrate of interest into contact with the sapphire using a stepper motor with a net displacement of around 2-4 μ m to create a contact spot that is larger than the size of the laser beam. The saturation of increasing SFG signal with pressure confirmed that the contact spot was sufficiently large. We estimate that the contact pressure achieved for the hardsheet samples was around 50 MPa and that the contact pressure achieved for the bilayer samples was around 20 kPa. Two scans for each sample at a given condition were averaged, and three repeats of each substrate in contact were collected.

■ RESULTS AND DISCUSSION

Measuring the Shift of the OH Peak for Various Rough PMMA Substrates. Figure 1 shows the geometry used for the SFG experiments. A rough poly(methyl methacrylate) (PMMA) sheet is placed in contact with a

sapphire prism. We roughened the PMMA sheets by rubbing 30-grit sandpaper for the roughest case, and we used a smooth PMMA sheet with root-mean-square (RMS) height roughness of around 10 nm as a control for a smoother surface. For reducing the modulus, we fabricated bilayer samples consisting of a stiff top layer of a 10- and 200 nm-thick PMMA layer on top of a soft elastomer, polydimethylsiloxane (PDMS). By choosing this design, we maintain the same chemistry in contact with the sapphire substrate and vary only the roughness or modulus. In addition to mechanical contact, we also spun-cast a PMMA solution in toluene on a sapphire prism and annealed the polymer film above its glass transition temperature to allow the interfacial molecules to orient in such a way as to attain maximum interactions with the surface OH groups. We expect these samples to highlight the differences between mechanical and optimum molecular contact.

Figures 2a,b show the SFG spectra for the different PMMA substrates (Table 1 in the Methods section) in contact with

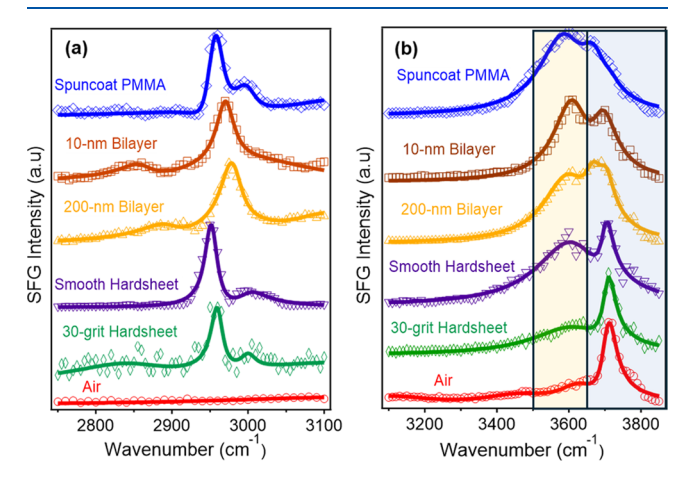


Figure 2. SFG spectra are for understanding the molecular contact between different PMMA substrates. The figure shows the raw spectra in PPP polarization (p-polarized SFG, IR, and visible beams) and fits to the data in (a) for the CH region (2750–3100 cm⁻¹) and (b) for the OH region (3100–3850 cm⁻¹). The shaded regions in (b) show the regions used for further analysis including the water region (white), the shifted OH region (yellow), and the free OH region (blue).

sapphire in both the hydrocarbon (CH) regions at 2750–3100 cm⁻¹ and the hydroxyl (OH) regions at 3100–3850 cm⁻¹. For comparison purposes, we also show the SFG spectra for the bare prism before contact ("Air"). The contact pressures for each sample were sufficient to make contact more than the

Table 1. Modulus and Root Mean Square Roughness Data for Different Substrates^a

Sample	Modulus	$h_{\rm rms}$ (Roughness)
10 nm Bilayer	1.0 MPa	2.5 nm
200 nm Bilayer	1.6 MPa	
Smooth Hardsheet	2.9 GPa ³²	8 nm
30-grit Hardsheet	2.9 GPa^{32}	1439 nm

^aThe elastic modulus for bilayer samples is calculated using the rule of mixture.^{29,30} The root mean square roughness for different PMMA substrates was extracted from the power spectral density of roughness, which was created using stylus profilometry and AFM scans across different length scales.³¹

overlapped beam size (diameter of about 100-200 μ m) (see the Methods section). The fits to the raw spectra (solid lines) in both regions were accomplished using the Lorentzian function, and the fitting parameters are listed in Table S1. The CH region shown in Figure 2a includes aliphatic vibrations from the chemical species present at the interface. The spectra for bare sapphire prisms have weak signals between 2800-3000 cm⁻¹, confirming the lack of hydrocarbon contaminants. Upon contact, we observe PMMA aliphatic signatures (i.e., vibrations of ester-methyl groups, α -methyl groups, and methylene). The characteristic peaks of PMMA observed across different samples include the symmetric vibration of the ester-methyl group at 2950 cm⁻¹ and the asymmetric vibration of the α -methyl group at 2995 cm⁻¹. The peak at 2960 cm⁻¹ corresponds to the asymmetric vibration of the backbone methylene signatures, as well as the α -methyl vibrations. Weak peaks in the 2850–2890 cm⁻¹ region correspond to the Fermi peaks of the ester-methyl groups.³⁴ These signatures confirm the presence of PMMA at the contact interface. In addition, the fits show distinct differences in the relative peak intensities of the characteristic peaks across different PMMA samples. The observation of different PMMA vibrations with differing intensities points toward the different local structures (conformations) adopted by the PMMA chains next to the surface. However, we can see that the relative aliphatic peak intensities are similar within the same group (spuncast, bilayers, and hardsheets). These differences in conformation would have direct implications for the molecules available for interaction at the surface, further affecting the molecular contact area. To quantify the orientation of PMMA side groups requires knowledge of the distribution of the orientation and the number density of these groups. We have used molecular dynamics (MD) simulations in past studies to determine the distribution of the orientation of PMMA side groups in contact with air.³⁵ Here, the width of the orientation distribution will be affected by both the roughness and molecular interactions. We have not attempted to quantify the orientation of PMMA side groups in this article and instead focused our analysis on the shift of the sapphire OH peak. In the future, we will use MD to assist us in the interpretation of the difference in methyl and methylene signals.

The region from 3100-3850 cm⁻¹ in Figure 2b shows the OH vibrations of the hydroxyl groups present on the sapphire interface. The air spectrum shows a sharp peak around 3710-3715 cm⁻¹ assigned to the free OH vibration of the sapphire hydroxyl. 36,37 On contact with PMMA substrates, these free hydroxyl vibrations shift to lower wavenumbers due to the acid-base interactions (hydrogen bonding is a subset of the broader category of acid-base interactions) with the functional groups in PMMA.^{37,38} The spectral features in Figure 2b directly illustrate the differences in contact between the rough and smoother sheets. The observation of a sharper unshifted peak at 3710-3715 cm⁻¹, which is similar to the spectral peak observed for the sapphire-air interface, confirms the presence of air gaps. For smoother and more compliant sheets, we observe the shift of this sharp peak to around 3670-3690 cm⁻¹ as well as an additional peak that is shifted to lower wavenumbers, illustrating the direct contact of molecular groups of PMMA with the surface OH groups. The peak at 3670-3690 cm⁻¹ reflects weaker interactions than we observed for sapphire OH in contact with methyl or methylene groups.²⁰ The higher shifted peak reflects stronger interactions with the carbonyl groups of the PMMA side chains.²³ Based on

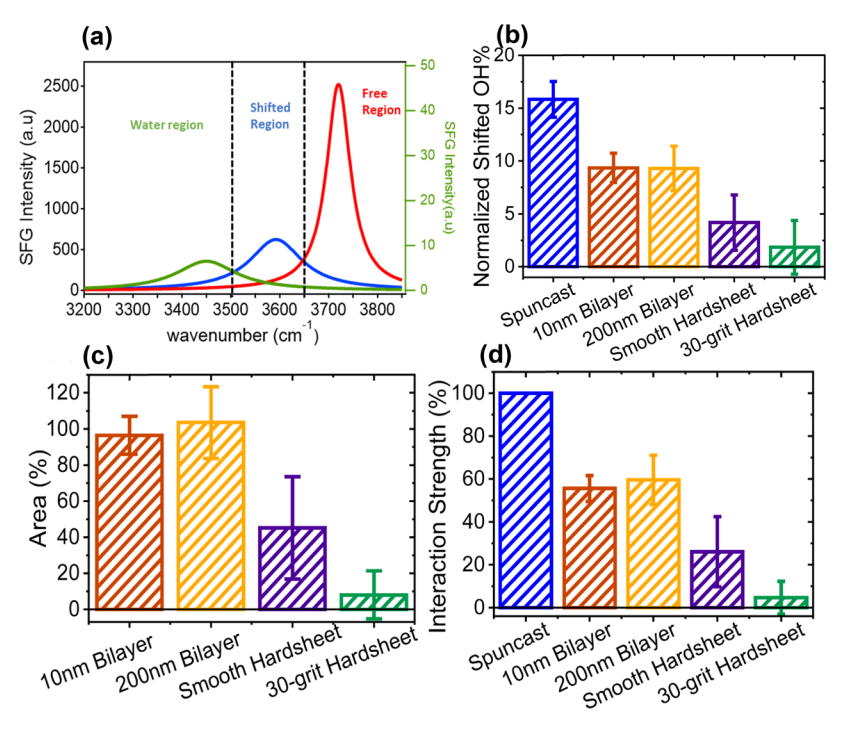


Figure 3. (a) Demarcation between different regions is based on the observed peak widths. The regions are defined by the intersection of the curves in green (a broad peak of loosely bound water at 3400 cm⁻¹), blue (a broad shifted hydroxyl peak due to molecular interactions), and red (a sharp free hydroxyl peak at 3700 cm⁻¹). The intersections around the wavenumbers take place at roughly around 3500 and 3650 cm⁻¹, which serve as the bounds for the analysis of *Shifted OH* %. Variation of (b) *Normalized Shifted OH* % parameter across different PMMA-based surfaces and (c) real contact area as a percentage of the nominal area calculated using *Shifted OH* %. By definition, the *Area* % of the Spuncast film is 100% since it is mechanically conformal but is not included in the figure to avoid confusion with the subsequent figure d and (d) interaction strength percentage as the percentage of the maximum possible interaction achieved at the contact interface for each system.

these observations, we observe that the rougher the PMMA sheet, the smaller the contact area. In addition, both the spuncast and bilayer films show the shifted OH vibrational peak with a lack of the free 3700 cm⁻¹ peak, suggesting complete coverage of the surface of the sapphire.

Converting the Shift of the OH Peak to Actual Contact Area. Next, we focus on converting the information about the shift in the OH peak to the contact area through an analysis of the shape of the hydroxyl region. We employ an area-under-the-curve method in which the hydroxyl region spectra are segregated into user-defined subregions that contain the maximum contribution from a given group but without introducing external bias. Different width and spectral feature observations across all samples were used for demarcating the regions shown in Figure 3a into free hydroxyl and weakly interacting PMMA moieties in the Free OH region (3650-3850 cm⁻¹, shown in blue), a strongly shifted region termed as the Shifted OH region (3500-3650 cm⁻¹, shown in yellow), and possible environmental adsorbed water accounted for in the water region (3100–3500 cm⁻¹, shown in white). In reality, each spectrum measured can in general exhibit multiple different peaks/populations of shifted OH signatures, but we grouped them all into a single spectral region of strong interactions called the Shifted OH region. For each region, the area is calculated from the square root of SFG intensity versus wavenumber since the square root of SFG intensity is the value proportional to the number of interacting molecules (Equation **S1**).

To extract information about the molecular contact area, we define a parameter termed *Shifted OH %* (eq 1) as the

percentage of the total OH region composed of the shifted OH signal.

Shifted OH % =
$$\frac{A_{shifted}}{A_{total}}$$
 (1)

Since we observe nonzero signals below 3650 cm⁻¹ in the air spectrum due to the presence of adsorbed water (Figure 2b), we observe that the Shifted OH % before contact is not zero. This presence of adsorbed water due to a humid environment can be observed (Figure 2b).³⁹ Thus, the nonzero Shifted OH % in the reference air spectra—which can generally vary between sapphire samples or under different levels of ambient humidity—necessitates the normalization of the Shifted OH % parameter for each sample using eq 2 to facilitate a better comparison between samples. The underlying assumption is that the same amount of adsorbed water is present before and after contact, which should be justified for a highly hydrophilic surface, such as sapphire. Finally, we add the caution that the calculated values, due to how the parameter is defined, are of a magnitude that is related to (but not directly equal to) the number of molecular contacts.

Normalized Shifted OH %

= Shifted OH
$$\%$$
(Sample) - Shifted OH $\%$ (Air) (2)

The calculated *Normalized Shifted OH %* (NSH) values for each of the different types of contacts are shown in Figure 3b. The results show decreasing values in the following order: Spuncast > Bilayers > Smooth Hardsheet > 30-grit Hardsheet. This decreasing trend is consistent with the qualitative observations that higher level of roughness and higher modulus

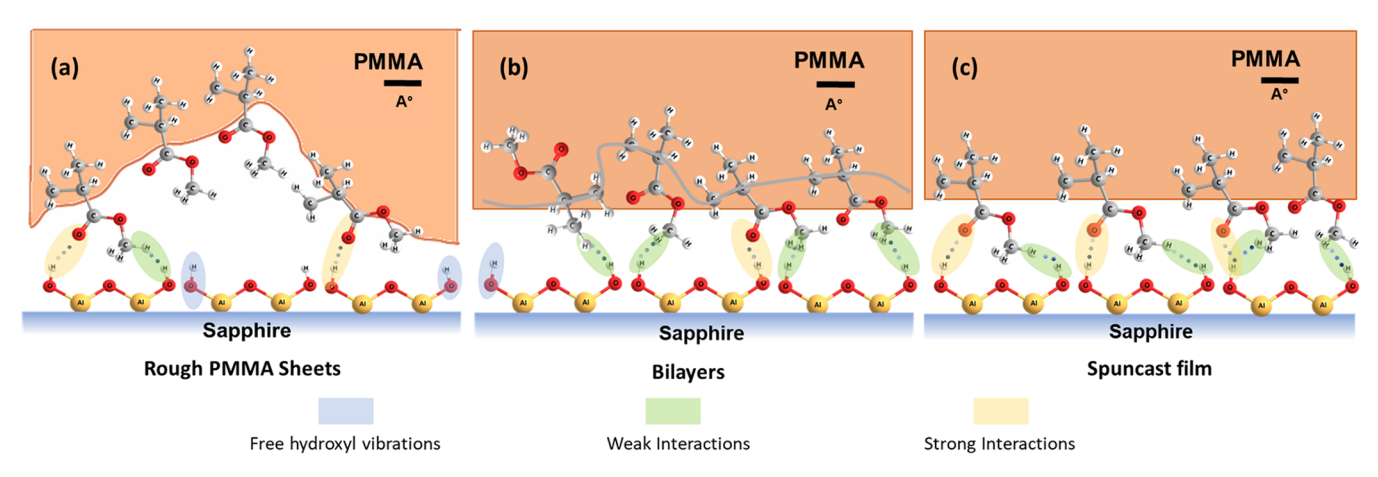


Figure 4. Proposed molecular contact picture drawn from the spectroscopic observations for the cases of (a) rough PMMA sheets, (b) bilayers, and (c) spun-cast PMMA film. The acid—base interactions of surface hydroxyl are denoted using different colors based on the type of interactions in increasing order from freely vibrating hydroxyl (*light blue*), weaker interactions with nonpolar groups (*light green*), and strong interactions with polar groups (*yellow*).

samples show lower values of *Normalized Shifted OH %*. This NSH serves as a comparative parameter derived from the SFG spectra between different systems.

Further, for transitioning from the NSH parameter to gauging molecular contact, we introduce a variable χ defined as the fraction of the area in direct contact. To determine χ , we need to define the Shifted OH % value for complete contact. We assume that the bilayer samples are conformal and are in complete contact with the sapphire substrate. This assumption is justified because we observed no changes in the values of Normalized Shifted OH % with applied pressure (Figure S1). This observation, alongside the lack of any discernible free hydroxyl peaks in the spectra for the two bilayer samples, suggests the possibility that both bilayer samples with a very thin layer of a stiff, glassy polymer are able to achieve conformal molecular contact. The fact that these bilayers will make conformal contact was not obvious, and our adhesion studies on bilayer samples with thickness of PMMA layer ranging between 0 and 100 nm revealed a drop in adhesion when PMMA thickness is around 80 nm.²⁸ This drop in adhesion was not due to a lack of conformability. Instead, the evidence that these systems are conformal was used to model the adhesion data by using the Persson-Tosatti model. This model predicts a drop in adhesion during approach because part of the adhesion energy is consumed in the elastic energy required to conform the PMMA layer to achieve molecular contact. 40,41 Further, due to the mechanically conformal nature of the bilayer, any nonconformal contact Shifted OH % can be expressed as a linear weighted sum of the Shifted OH % for complete contact (bilayer) and complete lack of contact (air).

However, an additional consideration needs to be made, given that the Fresnel factors are different for sapphire—air and sapphire—PMMA geometries. Figure S2 shows the square root of the SFG signals for the surface sapphire OH groups (based on Fresnel factors) expected as a function of the air gap thickness between the sapphire and PMMA at the chosen incident angle for our experiments. These changes in the SFG intensity have nothing to do with changes in orientation or changes in interaction energy. This is purely a correction factor due to Fresnel factors because the refractive index of the air gap is lower than PMMA and the SFG intensity of the surface OH groups will decrease with an increase in airgap thickness.

This results in changes in SFG intensity that we will observe for different regions in the nonconformal contact interface.

For the smooth samples with high contact pressure applied during the experiments, the signal contribution between the incontact and out-of-contact sites should be negligibly different since the scale of the out-of-contact air gaps will be very small (order of 10–15 nms). For the 30-grit hardsheet, the high $h_{\rm rms}$ values (Table 1) would lead to larger air gaps—creating substantial differences in signal contribution between the incontact and out-of-contact regions. Since the trend in Figure S2 reaches a bottom plateau past 700 nm, we can approximate that there will be a 2× relative signal enhancement for incontact sites (with an air gap of 0 nm) compared to out-ofcontact sites (>700 nm air gap). We define this correction factor to account for Fresnel factor as f and have taken this value as 1 for smooth PMMA surfaces and 2 for the 30-grit hardsheet. Using these two factors, we introduce eq 3 to determine χ , and then the Area % can be calculated by $\chi \times$ 100%. The denominator of eq 3 is a normalization factor for the sum of the coefficients before each Shifted OH % term to ensure that the addition of f changes only the relative contribution and not the overall magnitude.

Shifted OH % (measured)
$$= \frac{f \chi \times Shifted \ OH \ \%(contact) + (1 - \chi) \times Shifted \ OH \ \%(Air)}{f \chi + 1 - \chi}$$
(3)

The parameter *Area* % as shown in Figure 3c reflects the mechanical contact area considering the bilayer as the most conformal complete contact in eq 3. The higher the RMS roughness, the lower the *Area* %. The drop in *Area* % is almost exponential with an increase in the RMS roughness.

Explaining the Results for Spuncast PMMA Films. The final interesting observation to note is that the *Normalized Shifted OH %* for the spun-cast sample is 1.5 times higher than that for the conformal bilayer samples. While this finding might be presumed to be the result of the spuncast film conforming to a greater degree against the sapphire compared to the bilayers, this conclusion is not consistent with the pressureand thickness-dependent bilayer data, which suggests the conformality of the bilayer samples. Thus, the difference in these interactions cannot be related to changes in the contact

area. Instead, these differences reflect a difference in interfacial interaction energy for two instances of complete mechanical contact.

To account for these differences, we calculated the interaction strength percentage (Figure 3d) using eq 3 while considering spun-cast PMMA as the maximum possible contact (maximum interaction). While the PMMA in the bilayer samples may be in a kinetically locked nonequilibrium state, the PMMA that was spuncast and annealed directly on the sapphire surface should be at or near equilibrium with maximum interfacial interactions. We observe that despite the complete mechanical contact, the bilayer films have about a 50% decrease in the interaction strength percentage compared to that for the spun-cast PMMA, as shown in Figure 3d. Moreover, the rough sheets show a further decrease in the interaction strength due to the reduced mechanical contact at the interface, as shown in Figure 4a.

For the extreme case of a spun-cast film, the process of spin coating a polymer solution against the high-energy sapphire substrate allows for polymer chain to rearrange. Further, the annealing process ensures that a thermodynamically equilibrated state for the chains next to the interface is achieved.⁴² This equilibrated state and the presence of an abundance of polar groups maximize the interfacial interactions with the sapphire hydroxyl groups, as shown in Figure 4c. On the contrary, in the case of bilayers whose films experience an air environment, the local conformations of the polymeric chains try to minimize the surface energy by rearranging the nonpolar groups toward the surface as shown in Figure 4b. On mechanical contact with the sapphire prism, these available nonpolar groups at the surface are trapped in a kinetically favorable state next to the sapphire below their glass transition temperature T_g .⁴³ Thus, the reduced number of polar carbonyl groups reduces the interaction strength percentage for the bilayer as compared to that for the spuncast counterpart.

The observations presented above lead us to further consider the differences between conformal mechanical contact and the maximum interfacial interactions. Two systems that achieve complete coverage of sites at molecular length scales—the spuncast films and the bilayer contacts—have very different interaction energies that should, in turn, lead to differences in interfacial properties such as friction and adhesion. These intricacies are important to consider whenever the contact is achieved in different ways (e.g., mechanical contact as opposed to solution/melt) or when a material is processed at or above its $T_{\rm g}$ such that different degrees of molecular rearrangement can occur. This is a critically important detail when studying contact area, since interfacial interactions are ultimately what govern interfacial properties, and not every point of mechanical contact may yield the same interaction contribution even for the same material.

CONCLUSIONS

In our experiments using PMMA substrates with varying modulus and roughness in contact with sapphire with surface hydroxyls, we show the sensitivity of the shift in the location of the surface OH vibrational peak in the SFG spectra to the actual contact area between two rough solid surfaces. The higher the conformability, the lesser the magnitude of the free nonshifted OH peak. Here, we quantified the *Area* %, using the shifted OH vibrational peak. The results show that the higher the RMS roughness, the lower the *Area* %. The softer surfaces, which consist of a thin PMMA layer on top of a softer PDMS

sheet, show conformal contact and complete mechanical contact. Interestingly, we show that the interaction strength can be maximized even beyond complete mechanical contact, and the magnitude of the interaction strength depends on the orientation of groups at the surface of the contacting surface. The results for the interaction strength percentage highlight the distinction between two systems having complete contact: one via mechanical contact (bilayer) and the other using solution state (spuncast) contact that has been annealed above the $T_{\rm g}$. The importance of surface rearrangement combined with the impact of roughness is critical in understanding phenomena such as friction, adhesion, haptics, nanofabrication, and solid-state batteries, which are all driven by interfacial interactions that occur at molecular-scale contacts.

ASSOCIATED CONTENT

Supporting Information

The Supporting Information is available free of charge at https://pubs.acs.org/doi/10.1021/acs.jpcc.4c05287.

Dependence of the SFG intensity on the number of interacting species in contact. Table of Lorentzian fitting parameters for the aliphatic region of different PMMA contacts. Plot of NSH for the case of a bilayer with increasing pressure. Plot of calculated square root SFG intensity as a function of airgap thickness for a layer of air-separating sapphire and PMMA at the incident angle for the reported experiments (PDF)

AUTHOR INFORMATION

Corresponding Author

Ali Dhinojwala — School of Polymer Science and Polymer Engineering, University of Akron, Akron, Ohio 44325, United States; orcid.org/0000-0002-3935-7467; Email: ali4@uakron.edu

Authors

Utkarsh Patil — School of Polymer Science and Polymer Engineering, University of Akron, Akron, Ohio 44325, United States

Stephen Merriman — School of Polymer Science and Polymer Engineering, University of Akron, Akron, Ohio 44325, United States; orcid.org/0000-0001-9386-2774

Shubhendu Kumar — School of Polymer Science and Polymer Engineering, University of Akron, Akron, Ohio 44325, United States

Complete contact information is available at: https://pubs.acs.org/10.1021/acs.jpcc.4c05287

Author Contributions

[†]U.P., S.M., and S.K. contributed equally to this work. Conceptualization: U.P., S.M., S.K., A.D. Methodology: U.P., S.M., S.K., A.D. Investigation: U.P., S.M., S.K. Visualization: U.P., S.M., S.K. Supervision: A.D. Writing—original draft: U.P., S.M., S.K. Writing—review and editing: U.P., S.M., S.K., A.D.

Notes

The authors declare no competing financial interest.

ACKNOWLEDGMENTS

The authors acknowledge financial support for this work from the National Science Foundation (Award No. DMR-2208464). A.D. also acknowledges financial support from the Knight Foundation (W. Gerald Austen Endowed Chair). The authors thank E. Laughlin for custom device fabrication, P. Karanjkar for help with AFM, Chaitanya Gupta for help with the compression molding of the PMMA sheets, and G. Mallinos and V. Naiker for their help with SFG spectroscopy.

REFERENCES

- (1) Tiwari, A.; Wang, J.; Persson, B. N. J. Adhesion Paradox: Why Adhesion Is Usually Not Observed for Macroscopic Solids. *Phys. Rev. E* **2020**, *102* (4), No. 042803.
- (2) Israelachvili, J. N. Intermolecular and Surface Forces, 3rd ed.; Academic Press, 2011.
- (3) Yang, C.; Persson, B. N. J.; Israelachvili, J.; Rosenberg, K. Contact Mechanics with Adhesion: Interfacial Separation and Contact Area. *Epl* **2008**, *84*, 46004.
- (4) Tabor, D. Friction-the Present State of Our Understanding. J. Tribol 1981, 103 (2), 169–179.
- (5) Popova, E.; Popov, V. L. The Research Works of Coulomb and Amontons and Generalized Laws of Friction. *Friction* **2015**, 3 (2), 183–190.
- (6) Kogut, L.; Komvopoulos, K. Electrical Contact Resistance Theory for Conductive Rough Surfaces. *J. Appl. Phys.* **2003**, *94* (5), 3153–3162.
- (7) Shi, L.; Majumdar, A. Thermal Transport Mechanisms at Nanoscale Point Contacts. J. Heat Transfer 2002, 124 (2), 329–337.
- (8) Pratap, D.; Islam, R.; Al-Alam, P.; Randrianalisoa, J.; Trannoy, N. Effect of Air Confinement on Thermal Contact Resistance in Nanoscale Heat Transfer. *J. Phys. D Appl. Phys.* **2018**, *51*, No. 125301.
- (9) Krick, B. A.; Vail, J. R.; Persson, B. N. J.; Sawyer, W. G. Optical In Situ Micro Tribometer for Analysis of Real Contact Area for Contact Mechanics, Adhesion, and Sliding Experiments. *Tribol Lett.* **2012**, *45* (1), 185–194.
- (10) Li, L. T.; Liang, X. M.; Xing, Y. Z.; Yan, D.; Wang, G. F. Measurement of Real Contact Area for Rough Metal Surfaces and the Distinction of Contribution from Elasticity and Plasticity. *J. Tribol* **2021**, *143* (7), 1–5.
- (11) Rubinstein, S. M.; Cohen, G.; Fineberg, J. Contact Area Measurements Reveal Loading-History Dependence of Static Friction. *Phys. Rev. Lett.* **2006**, *96* (25), 1–4.
- (12) Li, L. T.; Liang, X. M.; Xing, Y. Z.; Yan, D.; Wang, G. F. Measurement of Real Contact Area for Rough Metal Surfaces and the Distinction of Contribution from Elasticity and Plasticity. *J. Tribol* **2021**, *143* (7), 1–5.
- (13) Benabdallah, S. M.; Lapierre, J. A New Device for Measuring the Real Area of Contact of Polymeric Material by the Perturbation of Total Internal Reflection. *J. Mater. Sci.* **1990**, *25* (8), 3497–3500.
- (14) Weber, B.; Suhina, T.; Junge, T.; Pastewka, L.; Brouwer, A. M.; Bonn, D. Molecular Probes Reveal Deviations from Amontons' Law in Multi-Asperity Frictional Contacts. *Nat. Commun.* **2018**, *9* (1), 888.
- (15) Hsu, C.-C.; Hsia, F.-C.; Weber, B.; de Rooij, M. B.; Bonn, D.; Brouwer, A. M. Local Shearing Force Measurement during Frictional Sliding Using Fluorogenic Mechanophores. *J. Phys. Chem. Lett.* **2022**, 13 (38), 8840–8844.
- (16) Petrova, D.; Weber, B.; Allain, C.; Audebert, P.; Venner, C. H.; Brouwer, A. M.; Bonn, D. Fluorescence Microscopy Visualization of the Roughness-Induced Transition between Lubrication Regimes. *Sci. Adv.* **2019**, *5*, No. eaaw4761.
- (17) Shen, Y. R. Basic Theory of Surface Sum-Frequency Generation. J. Phys. Chem. C 2012, 116 (29), 15505–15509.
- (18) Shen, Y. R. Fundamentals of Sum-Frequency Spectroscopy, 1st ed.; Press, C. U., Ed.; Cambridge, 2016.
- (19) Du, Q.; Superfine, R.; Freysz, E.; Shen, Y. R. Vibrational Spectroscopy of Water at the Vapor/Water Interface. *Phys. Rev. Lett.* **1993**, 70 (15), 2313–2316.
- (20) Nanjundiah, K.; Hsu, P. Y.; Dhinojwala, A. Understanding Rubber Friction in the Presence of Water Using Sum-Frequency Generation Spectroscopy. *J. Chem. Phys.* **2009**, *130*, 024702.

- (21) Bhatta, R. S.; Iyer, P. P.; Dhinojwala, A.; Tsige, M. A Brief Review of Badger–Bauer Rule and Its Validation from a First-Principles Approach. *Modern Physics Letters B* **2014**, 28 (29), No. 1430014.
- (22) Gaire, B.; Singla, S.; Dhinojwala, A. Screening of Hydrogen Bonding Interactions by a Single Layer Graphene. *Nanoscale* **2021**, *13* (17), 8098–8106.
- (23) Gaire, B.; Wilson, M. C.; Singla, S.; Dhinojwala, A. Connection between Molecular Interactions and Mechanical Work of Adhesion. *ACS Macro Lett.* **2022**, *11* (11), 1285–1290.
- (24) Wilson, M. C.; Singla, S.; Stefin, A. J.; Kaur, S.; Brown, J. V.; Dhinojwala, A. Characterization of Acid—Base Interactions Using Interface-Sensitive Sum Frequency Generation Spectroscopy. *J. Phys. Chem. C* **2019**, *123* (30), 18495—18501.
- (25) Narayanan, A.; Kaur, S.; Kumar, N.; Tsige, M.; Joy, A.; Dhinojwala, A. Cooperative Multivalent Weak and Strong Interfacial Interactions Enhance the Adhesion of Mussel-Inspired Adhesives. *Macromolecules* **2021**, *54* (12), 5417–5428.
- (26) Singla, S.; Wilson, M. C.; Dhinojwala, A. Spectroscopic Evidence for Acid–Base Interaction Driven Interfacial Segregation. *Phys. Chem. Chem. Phys.* **2019**, *21* (5), 2513–2518.
- (27) Dalvi, S.; Gujrati, A.; Khanal, S. R.; Pastewka, L.; Dhinojwala, A.; Jacobs, T. D. B. Linking Energy Loss in Soft Adhesion to Surface Roughness. *Proc. Natl. Acad. Sci. U. S. A.* **2019**, *116* (51), 25484–25490.
- (28) Kumar, S.; Gaire, B.; Persson, B. N. J.; Dhinojwala, A. Impact of Nanometer-Thin Stiff Layer on Adhesion to Rough Surfaces. *Phys. Rev. Res.* **2024**, *6* (3), No. 033015.
- (29) Hull, D.; Clyne, T. W. Introduction to Composite Materials, 2 ed.; Cambridge University Press: Cambridge, UK, 1996.
- (30) Yiu, P. M.; Yuan, H.; Gu, Q.; Gao, P.; Tsui, O. K. C. Strain Rate and Thickness Dependences of Elastic Modulus of Free-Standing Polymer Nanometer Films. *ACS Macro Lett.* **2020**, 9 (11), 1521–1526.
- (31) Gujrati, A.; Sanner, A.; Khanal, S. R.; Moldovan, N.; Zeng, H.; Pastewka, L.; Jacobs, T. D. B. Comprehensive Topography Characterization of Polycrystalline Diamond Coatings. *Surf. Topogr* **2021**, *9* (1), No. 014003.
- (32) Molero, G.; Tsai, C. Y.; Liu, C.; Sue, H. J.; Uenuma, S.; Mayumi, K.; Ito, K. Mechanical and scratch behaviors of polyrotaxane-modified poly (methyl methacrylate). *J. Appl. Polym. Sci.* **2021**, *138*, No. 51237.
- (33) Anim-Danso, E.; Zhang, Y.; Alizadeh, A.; Dhinojwala, A. Freezing of Water Next to Solid Surfaces Probed by Infrared-Visible Sum Frequency Generation Spectroscopy. *J. Am. Chem. Soc.* **2013**, 135 (7), 2734–2740.
- (34) Zhu, H.; Jha, K. C.; Bhatta, R. S.; Tsige, M.; Dhinojwala, A. Molecular Structure of Poly(Methyl Methacrylate) Surface. I. Combination of Interface-Sensitive Infrared-Visible Sum Frequency Generation, Molecular Dynamics Simulations, and Ab Initio Calculations. *Langmuir* **2014**, *30* (39), 11609–11618.
- (35) Zhu, H.; Jha, K. C.; Bhatta, R. S.; Tsige, M.; Dhinojwala, A. Molecular Structure of Poly(Methyl Methacrylate) Surface. I. Combination of Interface-Sensitive Infrared–Visible Sum Frequency Generation, Molecular Dynamics Simulations, and Ab Initio Calculations. *Langmuir* 2014, 30 (39), 11609–11618.
- (36) Du, Q.; Freysz, E.; Shen, Y. R. Surface Vibrational Spectroscopic Studies of Hydrogen Bonding and Hydrophobicity. *Science* (1979) **1994**, 264 (5160), 826–828.
- (37) Kurian, A.; Prasad, S.; Dhinojwala, A. Direct Measurement of Acid-Base Interaction Energy at Solid Interfaces. *Langmuir* **2010**, *26* (23), 17804–17807.
- (38) Wilson, M. C.; Singla, S.; Stefin, A. J.; Kaur, S.; Brown, J. V.; Dhinojwala, A. Characterization of Acid-Base Interactions Using Interface-Sensitive Sum Frequency Generation Spectroscopy. *J. Phys. Chem. C* **2019**, *123* (30), 18495–18501.
- (39) Boily, J. F.; Fu, L.; Tuladhar, A.; Lu, Z.; Legg, B. A.; Wang, Z. M.; Wang, H. Hydrogen Bonding and Molecular Orientations across

- Thin Water Films on Sapphire. J. Colloid Interface Sci. 2019, 555, 810-817.
- (40) Persson, B. N. J. Adhesion between Elastic Bodies with Randomly Rough Surfaces. *Phys. Rev. Lett.* **2002**, *89*, 245502.
- (41) Persson, B. N. J. Adhesion between an Elastic Body and a Randomly Rough Hard Surface. *Eur. Phys. J. E* **2002**, *8* (4), 385–401.
- (42) Li, X.; Lu, X. Interfacial Irreversibly and Loosely Adsorbed Layers Abide by Different Evolution Dynamics. *ACS Macro Lett.* **2019**, 8 (11), 1426–1431.
- (43) Kweskin, S. J.; Komvopoulos, K.; Somorjai, G. A. Molecular Restructuring at Poly(*n* -Butyl Methacrylate) and Poly(Methyl Methacrylate) Surfaces Due to Compression by a Sapphire Prism Studied by Infrared—Visible Sum Frequency Generation Vibrational Spectroscopy. *Langmuir* **2005**, *21* (8), 3647–3652.